ADVANCED MATERIALS
www.advmat.de

Synthesis and Applications of Graphdiyne-Based Metal-Free Catalysts

*Zicheng Zuo, Dan Wang, Jin Zhang, Fushen Lu, and Yuliang Li**

The development of carbon materials offers the hope for obtaining inexpensive and high-performance alternatives to substitute noble-metal catalysts for their sustainable application. Graphdiyne, the rising-star carbon allotrope, is a big family with many members, and first realized the coexistence of sp- and sp^2-hybridized carbon atoms in a 2D planar structure. Different from the prevailing carbon materials, its nonuniform distribution in the electronic structure and wide tunability in bandgap show many possibilities and special inspirations to construct new-concept metal-free catalysts, and provide many opportunities for achieving a catalytic activity comparable with that of noble-metal catalysts. Herein, the recent progress in synthetic methodologies, theoretical predictions, and experimental investigations of graphdiyne for metal-free catalysts is systematically summarized. Some new perspectives of the opportunities and challenges in developing high-performance graphdiyne-based metal-free catalysts are demonstrated.

1. Introduction

Catalysts are increasingly important cornerstones for the sustainable human development, with applications in, for example, the deep exploitation of solar energy, the efficient transformations of H_2O and CO_2, the environmental protection (e.g., consumption of CO, NO_x, and SO_x), and the energy-conversion technologies (e.g., Li–O_2, fuel cells).[1–5] Precious metals (e.g., Pt, Pd, Au)[6] dominate the commercial fields on account of their high catalytic activities, especially when applied in promoting the next-generation energy-conversion technologies. The huge demand for these noble-metal catalysts is, however, impacted by their scarcity and relatively low stability. Accordingly, the search continues for developing metal-free and non-noble-metal catalysts as sustainable alternatives.[7–10] Although some remarkable performances have been reached in the non-noble-metal catalysts originating from the metal–organic frameworks (MOFs) and the transition-metal dichalcogenides, recent observations in the metal-free carbocatalysts have revealed the obvious advantages of using carbon materials as the promising substitutes for noble-metal catalysts in many fields,[4,11–13] particularly for their robustness, durability, and low cost. Nevertheless, difficulties remain in terms of understanding their catalytic mechanisms and scaling up their production,[14–16] because the control over the molecular structures of carbocatalysts can be challenging, especially with regard to defects. Significant improvements in the performance and reproduction must be achieved if carbocatalysts are to realize practical applications.

The preparation of new carbon allotropes offers new opportunities for accelerating the development pace of high-performance carbocatalysts. The periodic connections among carbon atoms with a sole hybridization state have already produced diamond (sp^3), fullerenes (sp^2), carbon nanotubes (sp^2), and graphene (sp^2),[17] which have remarkably diverse mechanical and electronic properties: from soft to hard, and from insulative to conductive. Each of these carbon allotropes has contributed significantly to many interdisciplinary fields, including energy, catalysis, biology, and medicine.[17–19] Notably, the properties and achievements of those carbon materials are primarily originated from carbon atoms having one hybridization state. The question arises: might a carbon material comprising two hybridized states (sp and sp^2) function as a promising carbocatalyst?

Less than a decade ago, little was known about the properties of 2D carbon materials composed of the sp- and sp^2-hybridized carbon atoms with a nonuniform electronic distribution.[20–22] In 2010, graphdiyne (GDY), an atom-thick sp- and sp^2-hybridized all-carbon material, was the first all-carbon material prepared in a solution under mild conditions;[20] since then, it

Dr. Z. Zuo, Prof. Y. Li
Beijing National Laboratory for Molecular Sciences (BNLMS)
CAS Research/Education Center for Excellence in Molecular Sciences
CAS Key Laboratory of Organic Solids
Institute of Chemistry
Chinese Academy of Sciences
Beijing 100190, P. R. China
E-mail: ylli@iccas.ac.cn
Prof. D. Wang
Institute of Process Engineering
Chinese Academy of Sciences
Beijing 100190, P. R. China
Prof. J. Zhang
College of Chemistry and Molecular Engineering
Peking University
Beijing 100871, P. R. China
Prof. F. Lu
Department of Chemistry and Guangdong Key Laboratory
for Preparation and Application of Ordered Structural Materials
Shantou University
Guangdong 515063, China
Prof. Y. Li
University of Chinese Academy of Sciences
Beijing 100049, P. R. China
The ORCID identification number(s) for the author(s) of this article can be found under https://doi.org/10.1002/adma.201803762.

DOI: 10.1002/adma.201803762

has received wide attention for its promising applications in many fields, including solar cells, electrochemical actuators, radiation protection, solar steam generation, batteries, and catalysis.[23–29] As a rising-star 2D material, it is inspiring many traditional and new fields of research,[26,30,31] due to its porous nature, nonuniform electronic structure, and controllable all-carbon framework. In terms of the synthetic methodologies used to construct all-carbon materials, the homocoupling reaction under mild conditions for the preparation of GDY is the most readily one, and can be economically scaled up.[32,33] As a result, the GDY is highly controllable in terms of its primary structures and physical and chemical properties.[34,35] GDY should, therefore, be a valuable complement to prevailing sp^2-hybridized carbon materials; its structure rich in sp-hybridized carbon atoms offers many new insights into the construction of new-concept and highly active metal-free catalysts and in understanding their catalytic mechanisms. Here, we discuss systematically the superior properties of GDY in precisely controlling the molecular structures and the bandgap for catalysts, and summarize the recent theoretical and experimental achievements of GDY-based metal-free catalysts. We also provide a brief perspective on the challenges and opportunities while attempting to take full advantage of GDY in constructing highly efficient metal-free catalysts.

2. Synthesis of GDY Family Members

GDYs are members of a big carbon family. In general, GDYs are conjugated materials having a periodic array of diacetylene linkages in a 2D plane. **Figure 1**a summarizes the expanse of the GDY family members, and illustrates a universal strategy for their constructions. Following the synthetic methodology, it is possible to prepare many well-defined GDY-based materials through the homogenous coupling reaction, providing carbocatalysts many possible options. On account of the confined environments at solid–liquid or liquid–liquid interfaces, the resulting as-prepared samples generally possess superior 2D features and continuity.[37,42,43] A high-quality 2D structure is optimal for realizing the predesigned performance of a GDY-based material as the carbocatalysts.

The success polymerization of hexaethynylbenzene (HEB) on Cu foil, reported by our group in 2010,[20] opened the door to the possibility of preparing GDY-based materials readily. Many pioneering investigations into the preparation methodologies were performed to determine suitable catalysts (Figure 1b), temperatures, solution systems (Figure 1c), and substrates.[23,36,44,45] Adopting these approaches, the morphologies of GDYs can be highly controllable, with the nanofilms,[37] ultrathin nanosheets,[36] nanowalls,[45] nanotubes,[46] and nanochains[47] all readily prepared for on-demand applications. In general, these interesting morphologies have the necessary features for applying GDYs as high-performance metal-free catalysts or catalyst supports. Since these primary studies, many new GDY family members have been obtained through variations of the structures of the aromatic units and the number of acetylene groups (Figure 1a). For example, Huang's group employed H- and Cl-substituted precursors with three coupling positions to synthesize GDY films having nanoporous morphologies[38,48] (Figure 1d). These nanoporous structures, combined with the original in-plane molecular pores, formed a hierarchical structure—a promising anode material—that allowed the rapid migration of Li^+ and Na^+ ions. The content of sp-hybridized carbon atoms determines the reactivities, electronic properties, in-plane pore sizes, and mechanical properties.[49,50] Using this synthetic methodology, the content of the sp-hybridized carbon atoms is readily controlled. The highest content of sp-hybridized carbon atoms—up to 80%—has been realized in the system of β-GDY[39,51] (Figure 1e), and the lowest content of sp-hybridized carbon—up to 40%—has been obtained in the system of triphenylene-cored GDY[40] (Figure 1f,g). Furthermore, its low-temperature synthesis makes GDY the carbon allotrope that can most easily be doped with heteroatoms, which can thereby function as catalytic spots. As reported in Shang, Kan, and Huang's papers, N and B atoms have been introduced into the precursors, resulting in well-defined heteroatom-doped GDY derivatives[41,52–55] (Figure 1h,i). The well-defined configurations of the heteroatoms in these GDY compounds make it possible to precisely identify the catalytic mechanisms of such materials. Meanwhile, the traditional heteroatom-doping processes performed under high temperatures are also applicable in the GDY-based materials.[56,57] Similar to the sp^2-hybridized carbon materials, it is, however, difficult to control the configuration of the heteroatoms in the GDY materials when using these methods.

Zicheng Zuo received his doctorate degree in Prof. Yuliang Li's group at ICCAS in 2011. Then he worked at the University of Texas in Austin as a post-doctoral researcher. He is now an associate researcher in Prof. Yuliang Li's group. His research interests focus on the synthesis of graphdiyne-based materials, and investigating their applications in energy-conversion technologies.

Yuliang Li is a professor at the Institute of Chemistry, Chinese Academy of Sciences. His research interests lie in the fields of design and synthesis of functional molecules, self-assembly methodologies of low dimension and large-size molecular aggregations, chemistry of carbon and rich carbon, with particular focus on the design and synthesis of photo-, electroactive molecular heterojunction materials and nanostructured materials.

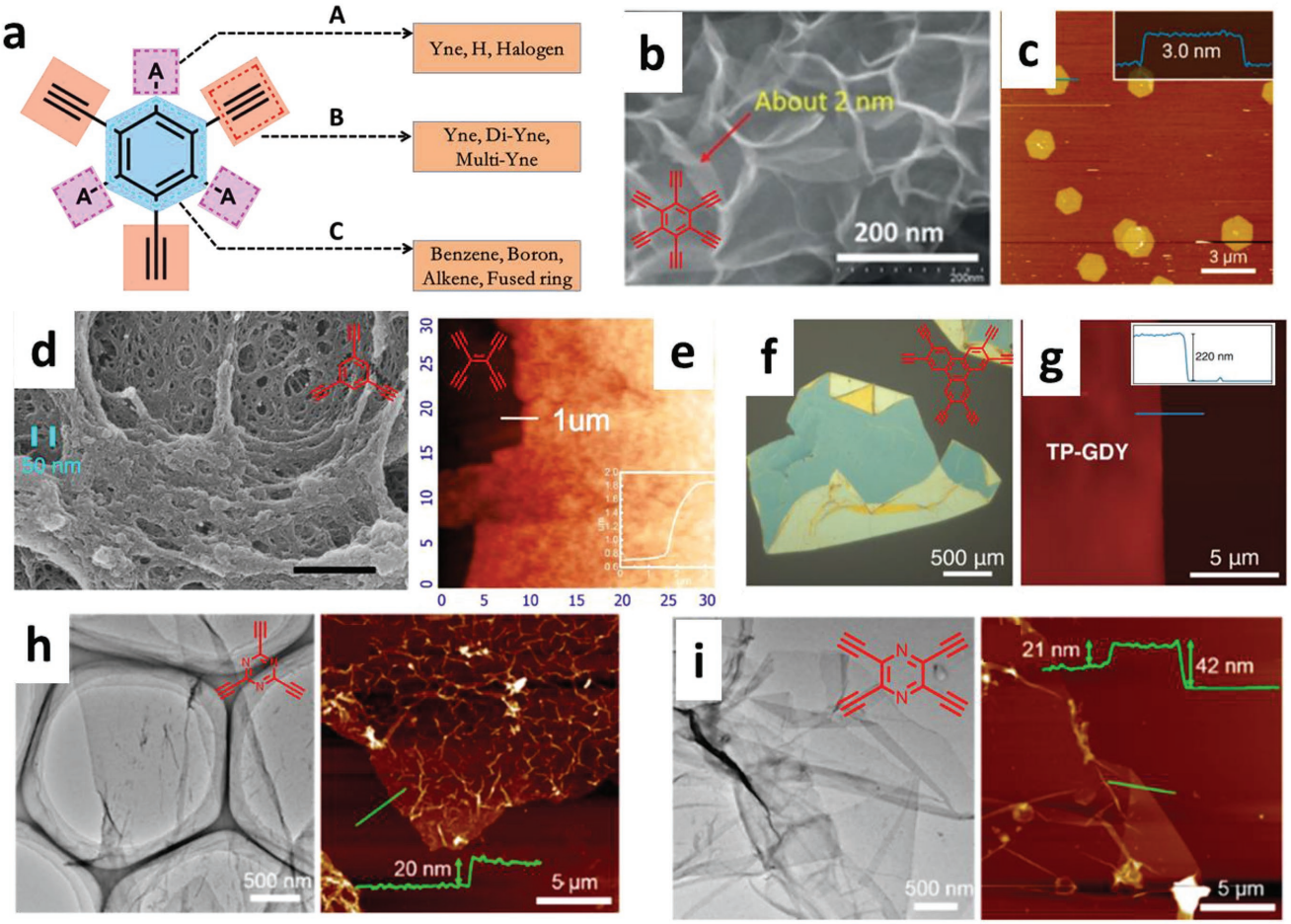

Figure 1. a) Structural engineering of GDY family members; b) SEM image of the large-scale ultrathin GDY nanosheets prepared using Cu nanowires. a,b) Reproduced with permission.[36] Copyright 2018, Wiley-VCH. c) AFM topographic image of hexagonal GDY nanosheets prepared at a gas–liquid interface. Reproduced with permission.[37] Copyright 2017, American Chemical Society. d) SEM image of a hydrogen-substituted GDY. Reproduced with permission.[38] Copyright 2017, Nature Publishing Group. e) AFM image of carbon ene–yne on a Cu foil. Reproduced with permission.[39] Copyright 2017, Elsevier. f,g) A fused-ring substituted GDY. f,g) Reproduced with permission.[40] Copyright 2018, American Chemical Society. h,i) Precisely N-doped GDY films. h,i) Reproduced with permission.[41] Copyright 2018, American Chemical Society.

3. Bandgap Engineering

The structures of GDY nanosheets have been characterized in detail.[58,59] Combining data from the high-resolution transmission electron microscopy (HRTEM) and selected-area electron diffraction (SAED) images with the results of theoretical simulations, it is demonstrated that the ABC stacking model is adopted in multilayer GDY[37,58] (**Figure 2**a). The progress in the structure of GDY paves the substantial way for the theoretical predictions. As a special 2D carbon allotrope, GDY has interesting electronic properties. Theoretical calculations have suggested that single-layer GDY is a semiconductor with a bandgap of 0.46 eV, close to the experimental findings,[66] and the electron mobility is on the order of 10^5 cm^2 V^{-1} s^{-1} and hole mobility approximately an order of magnitude lower[67] (Figure 2b). Compared with traditional sp^2-hybridized carbon allotropes, the GDY offers many possibilities for tuning the bandgap and carriers mobilities through the chemistry of its reactive triple bonds.

For many reactions in the energy- and environment-related fields, promoting the reduction and oxidation processes are the fundament assignments for the catalysts. The bandgap determines the responses of a material to the external stimulus (light, electric). The conduction band and valence band of the catalysts, respectively, play significant roles in directly impacting the reduction and oxidation processes and the catalytic mechanisms.[68] The band energy engineering of materials, thus, is the pivotal topic for improving the performance and efficiency of a catalyst.[2,68–71] Using the Vienna Ab Initio Simulation Package (VASP) and a projector augmented wave (PAW) method, Lee discovered theoretically that the bandgap of GDY could be varied efficiently through the addition of different number of hydrogen or halogen atoms[61] (Figure 2c). These hydrogen and halogen atoms added preferentially to the sp-hybridized carbon atoms, rather than the sp^2-hybridized carbon atoms, demonstrating theoretically the preferential reactivity of the triple carbon bonds in GDY. The introduction of these guest atoms to the triple bonds led to the successive transitions of the

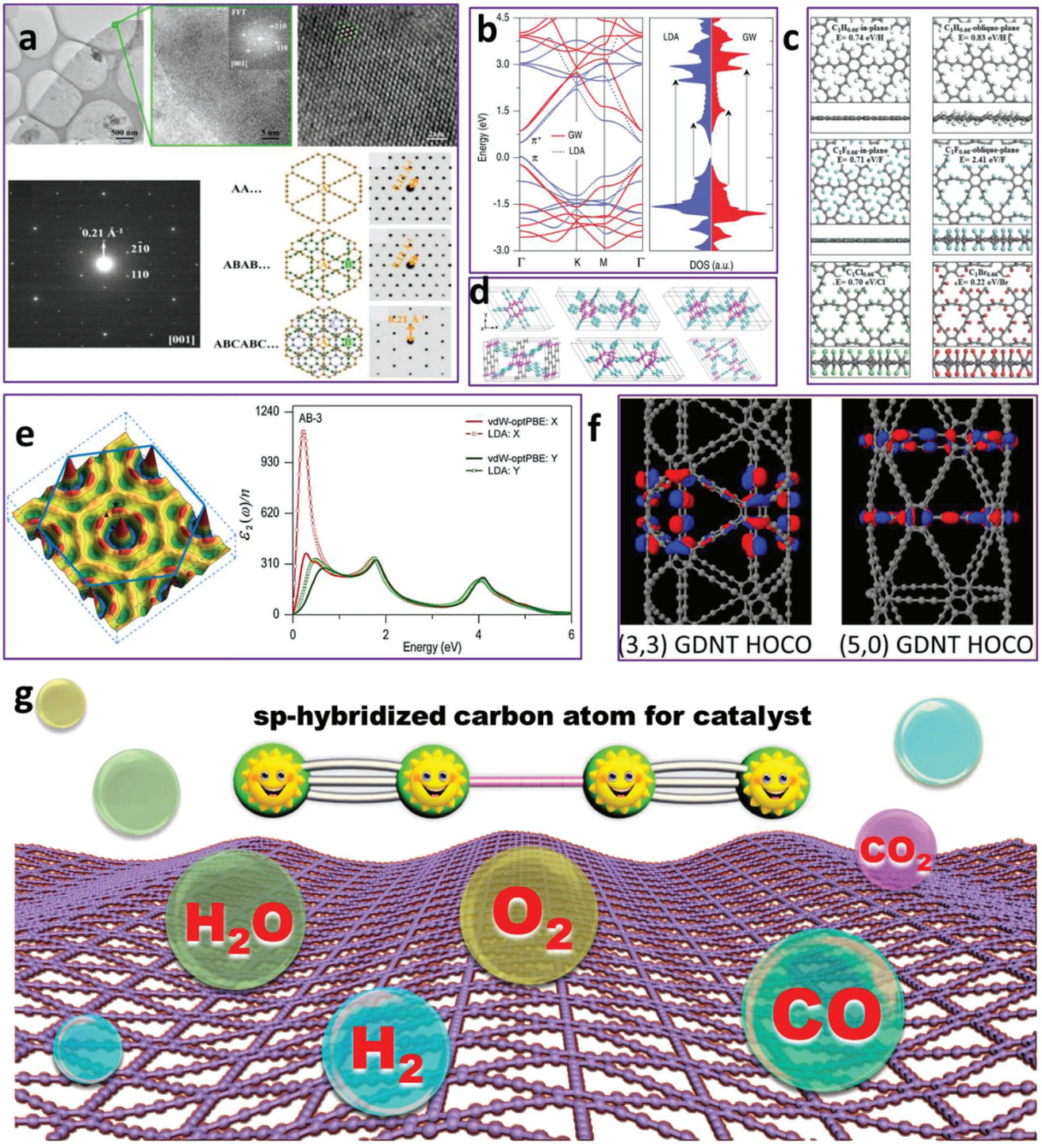

Figure 2. a) Direct TEM imaging of the crystal structure of a GDY nanosheet, and its stacking mode. Reproduced with permission.[58] Copyright 2018, Springer. b) Band structures and density of states (DOS) of GDY determined at the LDA and GW levels. Reproduced with permission.[60] Copyright 2011, American Physical Society. c) Bandgaps of GDY after accommodating hydrogen or halogen atoms. Reproduced with permission.[61] Copyright 2014, Royal Society of Chemistry. d) Possible interlayer crosslinking in GDY for band structure variation. Reproduced with permission.[62] Copyright 2015, Elsevier. e) Comparison of the dielectric function ($\varepsilon_2(\omega)/n$) along the *x*- and *y*-directions between the vdW-optPBE and LDA data for the stacked GDY; inset: total energy surface of bulk GDY with respect to the in-plane shift between the two layers. Reproduced with permission.[63] Copyright 2013, American Chemical Society. f) Highest occupied and lowest unoccupied crystal orbitals (HOCO and LUCO, respectively) for the (5,0) armchair and (3,3) zigzag tube configurations. Reproduced with permission.[64] Copyright 2016, American Chemical Society. g) Potential catalytic applications of the sp-hybridized carbon atoms of GDY.

sp-hybridized carbon to the sp^2 and sp^3 ones, resulting in dramatical variations in the conjugation degree. Thus, the bandgap of the GDY could be impacted greatly, from 0.5 to 5.2 eV. The in-plane and oblique-plane absorptions of these atoms on the carbon framework contributed diversely to the bandgap, with the oblique-plane configuration providing a higher bandgap. Notably, tailoring the bandgap of graphene remains a challenge because the introduction of defects shows lower controllability. Bandgap engineering is an important topic for the development of any catalyst, as well as for the construction of heterojunctions. These theoretical results pointed out the pathways for tuning the bandgap of GDY via the reactivity of its triple bond.[72]

Carbon–carbon triple bonds are highly reactive, and the well-arranged diacetylenes can be crosslinked intermolecularly under pressure, light, or elevated temperature.[73–76] GDY has many well-ordered diyne linkages in its structure, with a short distance between neighboring planes because of the strong π–π interactions. Therefore, it is possible that neighboring diacetylenes crosslink together under pressure, or some other external stimulus, to form a 3D interlinked framework. Xu and Gao used first-principles methods to calculate the special 3D carbon networks (so-called "GDY polymers") that would be originated from the crosslinking of GDY nanosheets.[62,77] Depending on the approaches, the as-prepared 3D structures were named Tri-C 18, Hex-C 36, Tri-C 54, and Orth-C 72 (Figure 2d). These new carbon allotropes were constituted by interlinked sp^3-hybridized carbon pillars and sp^2-hybridized graphene-like nanoribbons. These GDY polymers were predicted to be more energetically stable than the fullerene and GDY. The band structures were calculated using the LDA and HSE06 methods, and it was revealed the semimetallic properties for the polymer Tri-C 18. In contrast, Hex-C 36, Tri-C 54, and Orth-C 72 all had narrow direct (or quasi-direct) bandgaps, in the range from 1.55 to 1.74 eV. Thus, the bandgap of GDY can be tuned through the 3D crosslinking reactions. The 3D crosslinking would not only change the bandgap of GDY but also increase its mechanical strength, hardness, and Young's modulus (up to ≈1 TPa) along the direction perpendicular to the GDY nanosheets.[72]

Lu and Nagase found that the interlayer van der Waals interactions influenced the structural, electronic, and optical properties of GDY (Figure 2e).[63] These interactions directly impacted the stacking of GDY nanosheets, dramatically affecting the bandgap and producing the transition from a semiconductor to a metal.[63] The chirality and diameter of GDY nanotubes would also greatly change the bandgap and conductivity, with zigzag tubes having wider valence and conduction bands—and, thereby, presumably higher mobility for electrons and holes—than the armchair tubes[64] (Figure 2f). Similar to the prevailing sp^2-hybridized carbon materials, heteroatom-doping strategies would tailor the bandgap of GDY efficiently. Zhao introduced[65] boron (B) and nitrogen (N) elements as heteroatoms into GDY nanosheets. Theoretical predictions suggested that substitutions of N and B atoms into GDY would be easier than that into sp^2-hybridized carbons. The bandgap would vary largely, from 0.53 to 4.39 eV, according to the doping degree and the heteroatom configurations. Thus, the advantages of graphdiyne in the molecular and electronic controllability reveal its great promises for using as the metal-free catalysts in the energy and environment fields (Figure 2g).

4. Theoretical Predictions of Catalytic Behaviors

The oxygen reduction reaction (ORR) is a significant process in many high-energy-density devices, including fuel cells and metal-air batteries.[78] Many efforts were being made to boost the efficiency of the ORR, because the use of noble-metal-based catalysts is unsustainable for realizing inexpensive energy sources and, additionally, these noble-metal catalysts exhibit poor long-term stability. The metal-free carbon catalysts for the ORR have experienced much progress. Indeed, metal-free carbon catalysts have great promise as substitutes for noble-metal catalysts because of their inherent stability, low price, and sustainability. Although some impressive improvements in performance have been realized during the last decade, based on many traditional sp^2-hybridized carbon materials, further efforts will be needed to develop new materials and pursue the competitive performance. GDY in particular offers many possibilities for realizing highly efficient catalysts for the ORR.

Several theoretical predictions have been made regarding the properties of heteroatom-doped GDY. In the framework of GDY, two main types of heteroatom configurations are possible: they can, respectively, substitute the sp- or sp^2-hybridized carbon atoms. Chattopadhyay and Kang performed[79–81] systematic calculations of graphyne and GDY materials to investigate the influence of heteroatoms on the ORR performance (**Figure 3**a–c). The sp-hybridized carbon atoms appeared to be the most preferable sites for N-doping; indeed, after doping, the N-containing defects were observed to be highly oxytropic epicenters for trapping the O_2 molecules[80] (Figure 3d). Monotonically exothermic reactions with a four-electron pathway were predicted for catalyzing the ORRs in the N-doped graphyne and GDY systems. Simulations of the protonation steps of O_2 were revealed that the fourth protonation step of O_2 was the rate-limiting one when using most of the N-doped graphyne and GDY materials. The intermediates from these N-doped catalysts exhibited a linear scaling relation, much like those of the prevailing materials (Figure 3c). Nitrogen- and boron-doped catalysts occupied the strong and weak binding legs, respectively, of the activity volcano, with the N-doped materials believed to have better onset potentials.

Chattopadhyay's group also investigated the potential performance of B-doped GDY catalysts for the ORR.[81] They calculated the formation energies of typical B-doping sites on these carbon frameworks. From the formation energies, they observed that B dopants were favored to form at sp^2-hybridized carbon atom sites and to be far more stable than those at any other sites. In the doped structures, the B atoms are positively charged and their neighboring C atoms negatively charged, thereby increasing the ionicity of the covalent B—C bonds. Strong bonding between B and C atoms through such mixed interactions provides the B atoms with greater affinity toward sp^2-hybridized carbon atoms than toward sp-hybridized counterparts. For the O_2 adsorption, the B dopants act as effective sites for anchoring O_2 molecules and facilitating the adsorption process. Furthermore, although the O_2 is adsorbed most strongly on the B atoms that replace sp-hybridized carbon atoms, these oxygen atoms would interact so strongly with the substrates and oxidize them, harmful for the ORR. For the oxygen evolution reaction (OER), the performance of B-doped graphyne

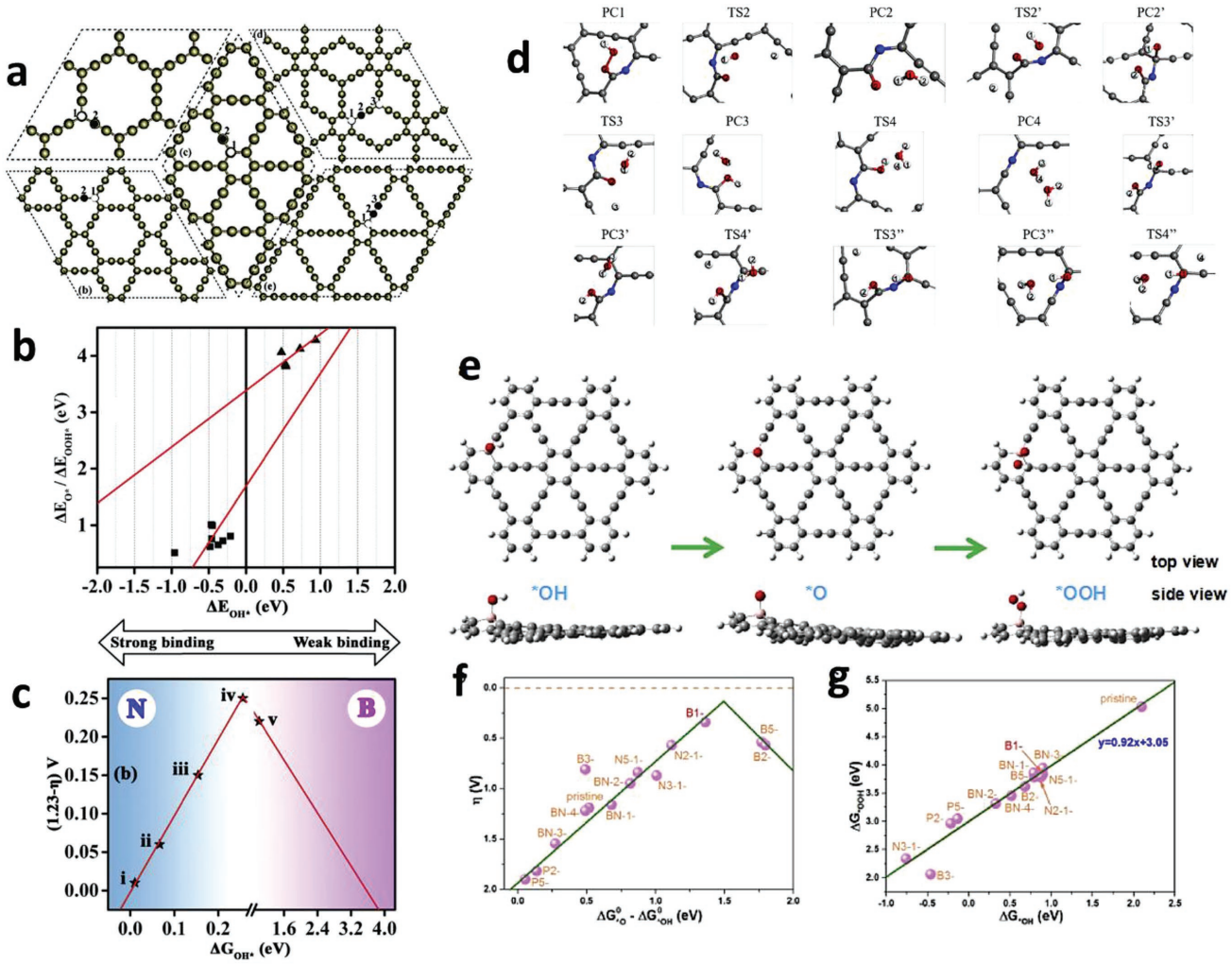

Figure 3. a) Possible N-doping positions in several sp-hybridized carbon-rich materials; b) adsorption energies of O* and OOH* plotted with respect to the OH* adsorption energy; c) onset potential plotted with respect to ΔG_{OH*} for these N-doped materials. a–c) Reproduced with permission.[79] Copyright 2016, Elsevier. d) Possible ORR process of the N1-βGy with the N replacing one sp-hybridized carbon atom. Reproduced with permission.[80] Copyright 2017, Elsevier. e) Steps in the oxygen evolution reaction (OER) on B-graphyne; f) volcano plot of the overpotential with respect to the universal descriptor $\Delta G(*O) - \Delta G(*OH)$ over various catalysts; g) linear relationship between the free energies of *OOH and *OH on graphyne-based catalysts. e–g) Reproduced with permission.[82] Copyright 2017, Elsevier.

in catalyzing the OER was predicted by Liu[77] (Figure 3e–g). The influence of B atoms in the local electronic/chemical environment of graphyne was calculated. It is suggested that the B atoms can improve the catalytic performance, especially on the occasion that the boron doping at edge sites. Thus, it can be inferred that the B-doped GDY would be efficient electrocatalysts for the water splitting and metal–air batteries.

The methods for the safe storage of H_2 will be key to its future applications.[83] Several metal hydrides, including $NaAlH_4$, $LiBH_4$, and $LiAlH_4$, are believed to be good media for safely storing H_2, due to the large gravimetric hydrogen content of these materials.[84] Nevertheless, the controlled release of H_2 from these highly stable compounds at low temperature has remained a challenge for many years.[85] Some new destabilization strategies will be necessary for the safe storage and use of H_2 in a society running on clean energy.[86] Compared with the behavior of metal-element dopants in these compounds, experimental and theoretical investigations have revealed that carbon nanomaterials with many curvatures might be potential "true catalysts" because: (i) the structures of these carbon frameworks are highly retainable for repeated reactions and (ii) strong interactions between the carbon nanomaterials and the light metals should favor a decrease in the H-removal energy. The interactions between the light metal atoms and the sp-hybridized carbon atoms in the GDY materials are, theoretically, stronger than those of the traditional sp^2-hybridized carbon nanomaterials;[87] exploiting this superiority might be a new way to anchor single metal atom for a high catalytic activity.[30,88,89] Song used density functional theory (DFT) methods with long-range van der Waals dispersion correction to examine the interactions between sp- and sp^2-hybridized carbon materials and light metal complex hydrides, including $LiAlH_4$, $LiBH_4$, and $NaAlH_4$[90] (**Figure 4**a–d). GDY and graphyne had much stronger interactions with the

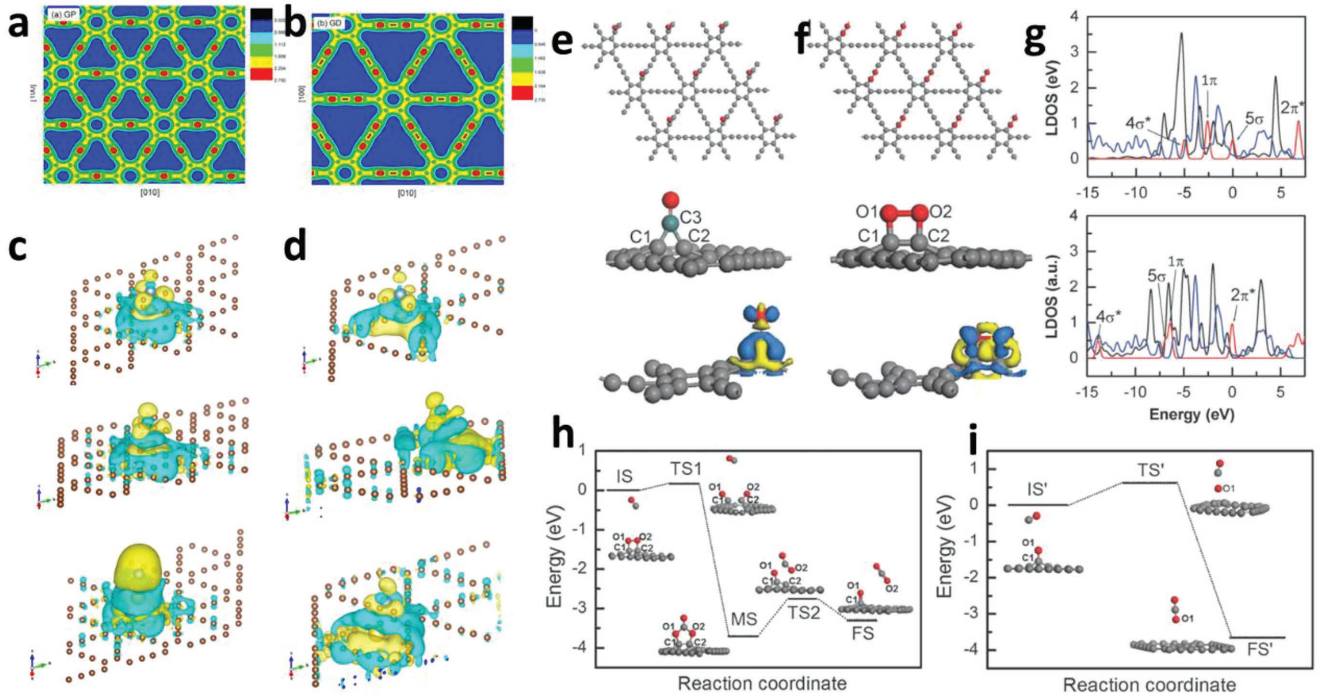

Figure 4. Graphyne and GDY catalyzing the release of hydrogen from metal complex hydrides: a,b) charge densities of the isolated graphyne and GDY on the (001) plane; c,d) isosurfaces with a charge density of 0.0025 when the metal complex hydrides of $LiAlH_4$, $LiBH_4$, and $NaAlH_4$ (from top down) were added to graphyne and GDY. a–d) Reproduced with permission.[90] Copyright 2013, American Chemical Society. GDY catalyzing the oxidation of CO: e,f) configurations and electron density difference maps (from top down) of CO and O_2 adsorbed on the GDY sheet; g) local density of states (LDOS) projected onto C—O (top) and O—O (down) on GDY; h,i) configurations of each state and minimum energy profiles in two different steps for CO oxidation reaction on the GDY sheet. e–i) Reproduced with permission.[91] Copyright 2014, Royal Society of Chemistry.

light metal atoms than did the fullerene, because they naturally featured many in-plane triangular cavities with the sp-hybridized carbon edges. Such strong interactions can remarkably affect the degree of charge donation from the alkali metal atom to the complexed AlH_4 or BH_4, thereby decreasing the strength of the Al—H or B—H bonds. Interestingly, for $LiBH_x$ complexes (x = 1–4), the presence of GDY or graphyne was remarkably beneficial for lowering the H-removal energy at all stages (as x decreased from 4 to 1), whereas it increased for $LiBH_4$ on the fullerene in the third stage. This observation suggests that the presence of sp-hybridized carbons might improve the efficiency of the dehydrogenation process. Therefore, the application of GDYs should inspire the revival of this old topic for safely and reversibly storing H_2.

Developing moderate approach for oxidizing the harmful CO is an important topic for improving the long-term durability of catalysts in fuel cells and solving environmental problems caused by CO emissions. The noble-metal-based nanocatalysts used at present are expensive, unsustainable, and can be easily poisoned by CO. Cai used DFT methods to theoretically investigate CO oxidation processes on a metal-free GDY backbone[91] (Figure 4e–h). Because of the π-conjugated network of sp- and sp^2-hybridized carbon atoms, the charge density on GDY is distributed nonuniformly. Mulliken charge density analysis revealed that electron transfer occurred from the sp-hybridized carbon atoms to the sp^2-hybridized carbon atoms in the benzene ring, causing the sp^2-hybridized carbon atoms in the ring to be negatively charged and the sp-hybridized carbon atoms in the diyne linkages to be positively charged. Thus, because the sp-hybridized carbon atoms were electron deficient, they might be the binding sites for O_2 and CO, facilitating the electron transfer from the absorbed molecules to the carbon network and enhancing the absorption. The feasible absorption and coadsorption of CO and O_2 on this novel electronic structure were deeply investigated. Energetically stable configurations of the adsorbates were formed only on the sp-hybridized carbon atoms; no absorption was found on the sp^2-hybridized carbon atoms. Two of the sp-hybridized carbon atoms in the GDY interacted with the carbon atom of CO, forming a triangular intermediate state—remarkably different from the absorption mechanism of metal-doped graphene, in which only a carbon–metal bond was formed between CO and a metal atom embedded in graphene.[92,93] In the intermediate state, ≈0.05 au of charge was transferred from GDY to CO, and occupied the antibonding CO-2π* orbital. Subsequently, the C—O bond was elongated from 1.14 to 1.22 Å. For the absorption of O_2, the absorbed O_2 was first aligned parallel to the GDY plane to form a tetrahedral intermediate structure with two sp-hybridized carbon atoms of a diyne linkage. During the formation of intermediate, ≈0.41 au of charge was transferred from the GDY plane to the O_2, and occupied the 2π* orbital of the O_2 unit. This process led to obvious elongation of the O—O bond from 1.22 to 1.49 Å, remarkably decreasing its strength. The absorption energy of O_2 on the GDY (–3.27 eV) was much higher than that of CO on GDY (–1.43 eV), therefore, the O_2 would mainly occupy the GDY surface if CO and O_2 coexisted in a system,

effective for resisting the CO poisoning.[94,95] The elongation of the O—O bond of the absorbed O_2 was ≈27.9%, implying a highly active state was achieved for oxidizing CO. Furthermore, the CO oxidation process catalyzed by GDY might follow the Eley–Rideal mechanism,[96] in which CO directly approaches an activated O_2 unit on the GDY and reacts with it. Importantly, the carbon–carbon bonds in GDY remain sufficiently strong during the reaction processes. These results demonstrate that GDY can be an effective, inexpensive, and metal-free catalyst for low-temperature oxidation of CO in fuel cells and for environmental applications.[88,89,97]

5. Experimental Investigations of GDYs as Metal-Free Catalysts

Developing highly efficient photocatalysts for the water splitting reaction would be a very sustainable technology for producing clean fuel (H_2, O_2) from the infinite supply of sunlight. Photocatalysts based on the prevailing inorganic semiconductors suffered severely from several problems: long-term instability, low quantum efficiency, and limited tunability of the bandgap. When compared with these inorganic photocatalysts, GDY-based materials would appear to be superior in terms of bandgap engineering and stability of carbon-rich frameworks. Therefore, the engineering strategies we described earlier for GDY materials should provide a great possibility for matching the bandgap energy and the quantum efficiency and, thereby, allowing the construction of highly efficient photocatalysts.

Wu reported two modified GDY materials—PTEPB and PTEB, obtained through polymerizations of the monomers 1,3,5-tris(4-ethynylphenyl)benzene and 1,3,5-triethynylbenzene, respectively—that were tested as metal-free photocatalysts for water splitting under visible light[98] (**Figure 5**). The as-obtained samples of PTEPB and PTEB were highly efficient photocatalysts for splitting neutral water, producing H_2 and O_2 stoichiometrically under visible light. When irradiated by the light of 420 nm, the apparent quantum efficiencies of PTEPB and PTEB reached up to 10.3 and 7.6%, respectively. When using the full solar spectrum, these photocatalysts delivered a solar-to-hydrogen conversion efficiency as high as 0.6%—about six times higher than that of photosynthetic plants in converting solar energy to biomass (global average: ≈0.10%). In contrast to the two-electron mechanism found in the C_3N_4-based catalysts, these GDY-based samples catalyzed the OER through a four-electron process. Theoretical simulations were performed using first-principles methods, and revealed the mechanisms behind the photocatalysis of the OER and the hydrogen evolution reaction (HER). Once these materials were doped with photogenerated holes, deprotonation processes on the surface were feasible because water molecules could be adsorbed chemically on the molecular backbones of PTEPB and PTEB, and a four-electron pathway was evoked for the OER. In contrast, the photogenerated electrons drove the HER via two one-electron transfer processes, corresponding to the formation of *H intermediates at the active sites. Photogenerated excitons located over various carbon atoms were calculated for their abilities to function as active centers for the evolution of H_2

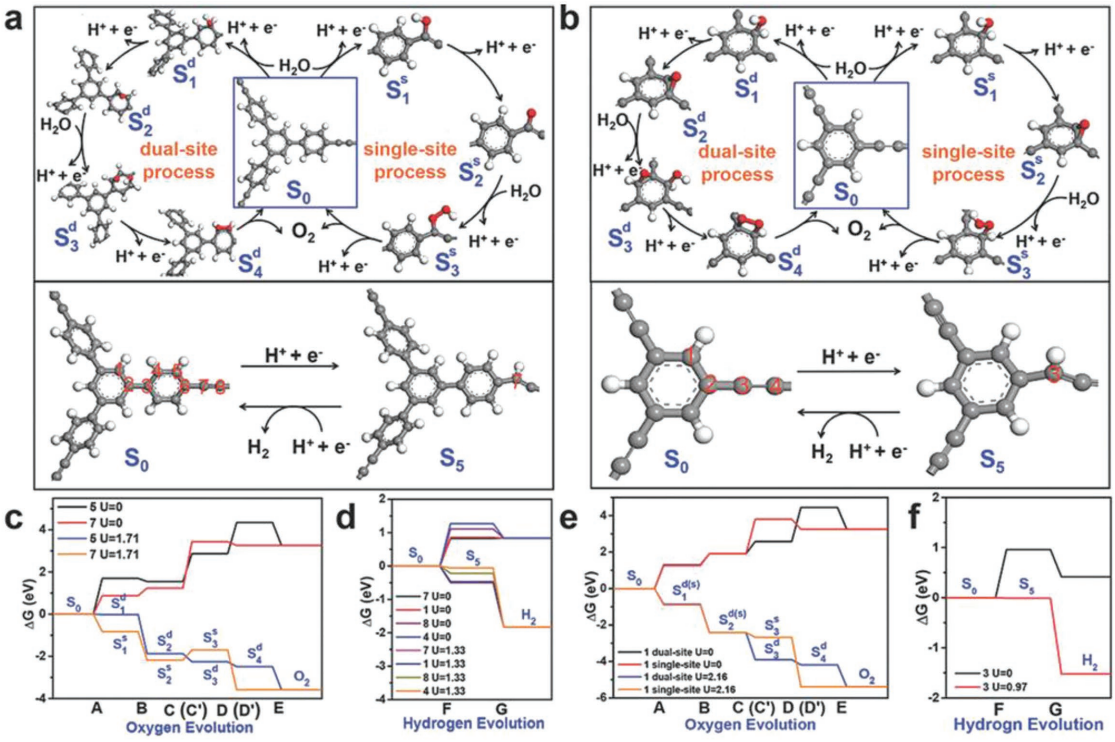

Figure 5. a,b) Proposed photocatalytic cycles of the oxygen evolution reaction (via single- and dual-site processes) and the hydrogen evolution reaction at the most feasible sites in both PTEPB and PTEB; c–f) Gibbs free energy changes (ΔG) for each step in the oxygen and hydrogen evolution processes on PTEPB and PTEB. Reproduced with permission.[98] Copyright 2017, Wiley-VCH.

and O_2. The activity of the sp-hybridized carbon atoms in these GDY-based catalysts was greater than that of the sp^2-hybridized carbon atoms. In a separate study, Zhang used DFT to investigate the active sites responsible for catalyzing the HER.[99] The carbon atoms of the benzene rings in PTEB were the dominant active sites for the photocatalytic H_2 evolution; sites 1 and 3 were favorable for single-site H_2 evolution, while sites 1 and 2 were favorable for dual-site H_2 evolution. After repeated visible-light photocatalytic tests, these photocatalysts, both based on GDY frameworks, remained highly stable, implying that their special structures (carbon-rich frameworks) could minimize charge build-up on their surfaces, thereby preventing photochemical degradation.

Bojdys and co-workers designed a triazine-containing precursor presenting three terminal acetylene units and investigated its growth properties on Cu foil.[100] Interestingly, the three terminal alkyne units of three precursors were first linked together to form benzene rings through copper-mediated [2 + 2 + 2] cyclotrimerization. The as-prepared polymer (TzF) exhibited good 2D property, with well-defined patterns observed using HRTEM, SAED, and scanning force microscopy (SFM), confirming the existence of a hexagonal unit cell, in agreement with the 2D hexagonal lattice parameters. TzG was subsequently constructed on the top of TzF film through the cross-coupling of the terminal alkyne units. A twinned mechanism was appeared to be responsible for constructing the TzF/TzG heterostructure. Through electrochemical testing, the bandgap of the bulk heterojunction was ≈1.84 eV; this value was in good agreement with the optical bandgap determined from the UV–vis absorption edge and photoluminescence spectroscopy. From comparisons with the DFT data, the optical and electronic bandgaps of the TzF/TzG heterostructure were closer to the bandgap energy of 3D TzG. This finding was indicative of a type I band alignment between TzF and TzG. The TzF/TzG heterostructure was then used as a metal-free photocatalyst for hydrogen evolution from water. In a water/acetonitrile mixture (1:1) at room temperature, this catalyst was irradiated with visible light at 395 nm, with triethanolamine as the sacrificial electron donor. The rate of hydrogen evolution in the absence of a Pt cocatalyst (34 μmol h^{-1} g^{-1}) was very close to that in the presence of a Pt cocatalyst (35 μmol h^{-1} g^{-1}). After testing, this photocatalyst remained stable, with no significant variations in its chemical behavior. The performance of the neat 2D TzF flakes was also tested, but no measurable hydrogen evolution was detected, confirming that the highest occupied molecular orbital (HOMO) of the GDY-based TzG was better matched with the hydrogen reduction potential than was the HOMO of 2D TzF.

Graphitic carbon nitride (g-C_3N_4) has received much attention for photocatalytic water splitting because it is a metal-free semiconductor possessing a suitable bandgap.[101–104] Nevertheless, the poor mobility of photoinduced holes severely restricts its photocatalytic performance. GDY was predicted to have a high hole mobility,[105] and its excellent hole mobility had been exploited to improve the performance of inorganic CdSe quantum dots and $BiVO_4$ photocathodes for hydrogen production.[106] Accordingly, Lu's group employed GDY to enhance the hole mobility of g-C_3N_4. In this concept, GDY nanowalls were used as an all-carbon framework upon which g-C_3N_4 was assembled in situ, thereby affording a metal-free 2D/2D g-C_3N_4/GDY heterojunction. This structure took full advantages of the high surface area, thinness, and 2D continuousness of the GDY component. Indeed, the uniform metal-free 2D/2D g-C_3N_4/GDY heterojunction was an efficient photoelectrocatalyst for water splitting; it improved the photocarrier separation due to the excellent hole transfer characteristics of GDY. Furthermore, in neutral aqueous solution, the special structure of the 2D/2D heterojunction increased the electron lifetime and the photocurrent density substantially, by sevenfold (to 610 μs) and threefold (to −98 μA cm^{-2}), respectively, at 0 V versus a normal hydrogen electrode (NHE). These improved characteristics were helpful in catalyzing hydrogen evolution. In addition, when this novel 2D heterojunction was loaded with Pt catalyst (Pt@g-C_3N_4/GDY), the performance was further enhanced, with the photocurrent reaching −133 μA cm^{-2} at a potential of 0 V versus NHE in a neutral aqueous solution.

GDY differs from prevailing carbon materials because it contains both sp- and sp^2-hybridized carbon atoms and features a nonuniform distribution of charge density at each carbon atom. The state-of-the-art thermal treatments for doping prevailing carbon materials are suitable for preparing heteroatom-doped GDY, potentially producing new heteroatom configurations for catalysis. When Zhang thermally treated GDY in the presence of NH_3 at temperatures from 400 to 600 °C,[57] the resulting N dopants had two different configurations, corresponding to imino (substitution of the sp-hybridized carbon atoms) and pyridyl N atoms (substitution of the sp^2-hybridized carbon atoms) (**Figure 6**a–c). Experimental analysis and first-principles calculations both concluded that the imino N atoms were formed primarily, because the sp-hybridized carbon atoms have higher activity and can be easily substituted by the N atom. The N-doped GDY had catalytic performance higher than that of the untreated sample. The sample treated at 550 °C had the best performance, with superior values for its onset potential, current density, and electron transfer number. Although, the catalytic activities of these samples were lower than that of a commercial Pt/C catalyst, this approach hinted that it might be possible to develop GDY-based metal-free catalysts with performance comparable to that of metal-based catalysts. Subsequently, Huang doped GDY with N-containing donors (pyridine, NH_3) at even higher temperatures[107] (Figure 6d–f). First, the porous GDY was immersed in pyridine for 3 d; the pyridine-saturated GDY was then washed and dried. The as-dried GDY was treated thermally at 700, 800, 900, or 1000 °C for 1 h, resulting in the GDY samples doped with small amounts of N atoms derived from adsorbed pyridine (named N-GDY-700 °C, N-GDY-800 °C, N-GDY-900 °C, and N-GDY-1000 °C, respectively). To increase the N-content in the GDY, the as-prepared GDY-900 °C sample was further calcined at 800 °C under an NH_3 atmosphere, providing a sample named N′N-GDY. The N atoms in the samples had some novel modes of substituting sp-hybridized carbon atoms. This N-doping strategy, which resulted in the novel configurations of imine N-2, imine N-2,2, and pyridinic N, was helpful for booming the catalytic activity of ORR in the alkaline condition. Impressively, the higher contents of N dopants in the sample of N′N-GDY led to the catalytic performance comparable to that of a commercial Pt/C catalyst (20%), and better than those of most other reported metal-free catalysts. Furthermore, when compared to

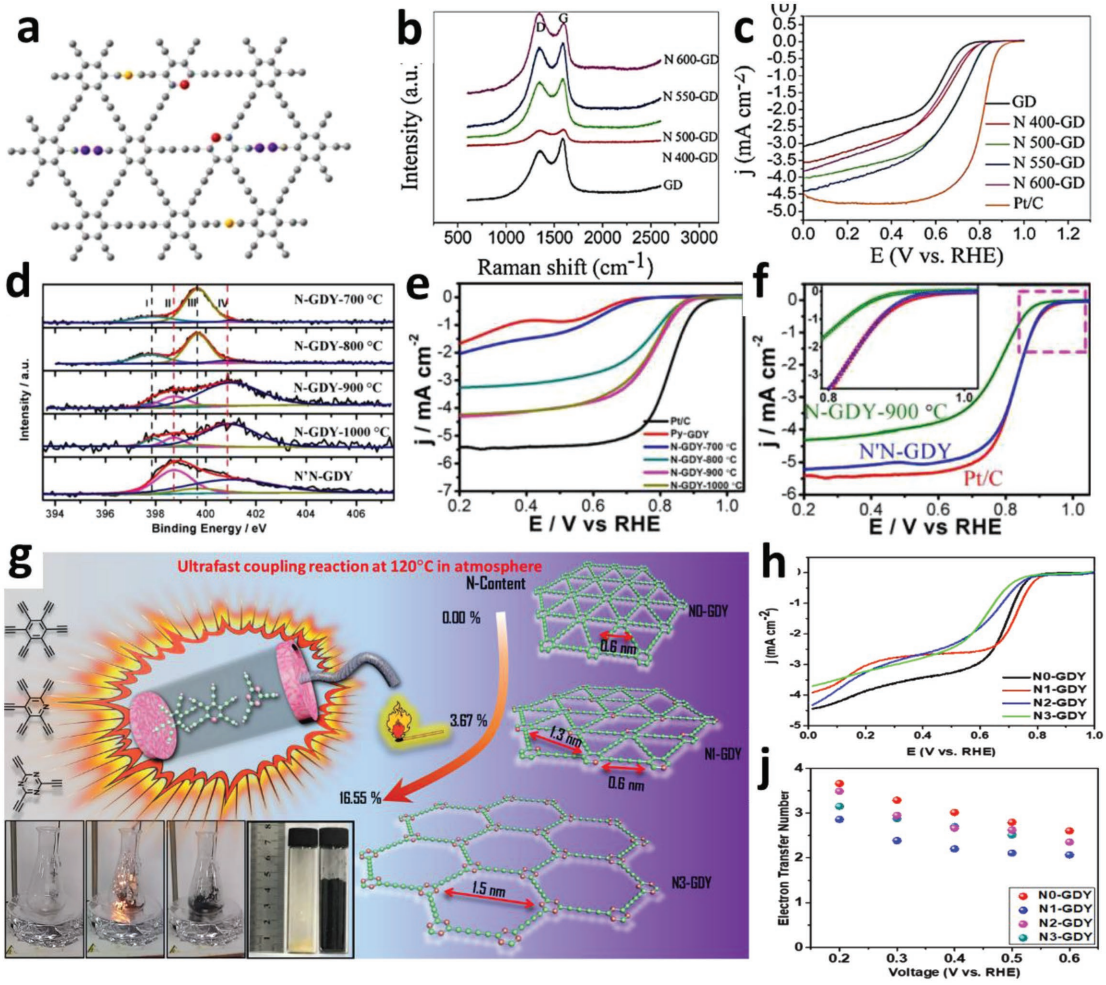

Figure 6. a) Possible structure of GDY doped through thermal treatment at temperatures from 400 to 600 °C; b) Raman spectra of the as-prepared samples and c) their corresponding performance in catalyzing the ORR under alkaline conditions. a–c) Reproduced with permission.[57] Copyright 2014, Royal Society of Chemistry. d) XPS patterns, e) electrochemical performance in catalyzing the ORR, and f) stability of N-doped GDY prepared through thermal treatment at temperatures from 700 to 1000 °C. d–f) Reproduced with permission.[107] Copyright 2017, American Chemical Society. g) The explosion method for preparation of N-doped GDY with a precise N-configuration, h) the electrochemical performance of these samples for catalyzing the ORR, and j) their electron transfer numbers in the ORR. g–j) Reproduced with permission.[53] Copyright 2018, Elsevier.

Pt-based catalysts, N-doped GDY would have better long-term stability, similar to that of other metal-free carbon catalysts.

Controlling the molecular structure of metal-free catalysts based on the prevailing sp^2-hybridized carbon materials remains a challenge.[108,109] Therefore, determining the precise mechanisms of a metal-free catalysts can be controversial, and the development of high-performance metal-free catalysts continues to be based on trial-and-error approaches. The appearance of GDY-based metal-free catalysts makes it possible to solve the controversies and, thereby, develop precise structural engineering strategies for the formation of highly active epicenters. Li's group developed an explosion method in air for constructing N-doped GDY nanochains with well-defined N-configurations[53] (Figure 6g–j). Using this bottom-up method, the N-configuration (pyridyl N atoms or triazine-like N clusters), N-contents (from 0 to 16.55%), and porous structures could be controlled precisely by varying the precursors, demonstrating the outstanding controllability of GDY. This method allows the efficient fabrication of useful GDY-based materials under simple conditions. Remarkably, this bottom-up approach for constructing N-doped GDY successfully avoids one major problem: producing well-defined N configurations without any metal impurities—a situation that has perplexed researchers of metal-free catalysts for many years. The as-prepared nanochain-like N-doped GDY could be dispersed well in solution, beneficial for the electrode fabrication. Measurements confirmed the influence of the N-dopant on the onset potential of the ORR: the pyridyl N atoms improved the onset potential to 0.87 V (vs RHE), 0.05 V higher than that for N0-GDY (0.82 V). The N-content was not the more the better, and the heavy doping by triazine-like N cluster slacked the ORR with the onset potential of 0.8 V, presumably because of decreased conductivity resulting from the lower degree of conjugation. The bare GDY functioned through a four-electron-dominated ORR pathway, and its electrocatalytic efficiency was superior to that of the N-doped sample. The introduction of the N atoms impaired the

electron transfer number. The presence of pyridyl N dopants in GDY led mainly to a two-electron-transfer ORR process, probably because of the single N active center in each unit. Because the triazine-like N clusters featured three active N atoms in each unit, they partially overcame this drawback; indeed, the electron transfer number was higher than that of N1-GDY over the whole potential range.

6. Conclusions and Perspectives

GDY-based carbon materials are becoming rising stars among 2D materials, with their impact growing gradually in many research fields. The ready preparation of these new sp- and sp^2-hybridized carbon materials is opening new windows for researchers, who seek for new structures with on-demand properties—a situation that does not exist for the prevailing carbon systems.[26,27,30,110–112] The uneven distribution of electrons in GDY is dramatically different from that in other well-studied sp^2-hybridized carbon materials, potentially resulting in the realizations of new properties and new-concept carbocatalysts. Indeed, many new opportunities and challenges are arising.

We have summarized the recent progress related to GDY-based metal-free catalysts in terms of the material synthesis, theoretical investigation, and electrochemical performance. GDY exhibits many superior aspects when compared with other carbon-based materials, including outstanding controllability in its molecular structure, bandgap, and processability. Both theoretical and experimental observations have suggested that huge new developments will occur from this new carbon family, particularly in developing high-performance metal-free catalysts and intrinsically understanding their catalytic mechanisms. Nevertheless, more efforts will be needed to fully comprehend the behaviors of GDY-based metal-free catalysts, from both the theories and experiments.

First, the synthetic methodologies for preparing GDYs should be systematically expanded. Unlike the sp^2-hybridized carbon materials, GDYs are members of a big carbon family. Thus, the synthesis of GDYs can encompass a wider range of techniques. A deep understanding of the synthesis of each member, in terms of thermodynamics and kinetics, will be necessary for preparing high-quality GDY materials in large scale. To date, only a few methods have been developed for synthesizing GDYs,[37,47,113–115] and the mechanisms behind their growth processes have yet to be clearly revealed.

In addition, more investigations will be needed to understand the chemical, electrochemical, and physical behaviors of the sp-hybridized carbon atoms in GDYs.[116] A structure rich in sp-hybridized carbon atoms is one of the most important features of a GDY. The responses of the sp-hybridized carbon atoms to external stimuli are fundamental to the materials' catalytic activities and stabilities. Such investigations should draw on the expertise gained from studying acetylene chemistry in organic synthesis.[32,74,117]

Furthermore, only limited efforts have been devoted to developing GDY-based metal-free catalysts, compared with the larger experimental undertakings related to the prevailing sp^2-hybridized carbon materials.[4,118–122] The latter has paved the way for the construction of more highly active carbocatalysts based on GDYs.[123,124] Specially, more interesting research will be focused on the catalytic kinetic and thermodynamics, performance stability, and antitoxic mechanism of the GDY-based metal-free catalysts, because GDY has a novel electronic structure and can be customizable. The achievements in this area would be applicable for other catalysts based on the noble-metal and non-noble-metal materials. Additionally, similar to the studies of sp^2-hybridized carbon materials, more powerful and effective characterization will be necessary if we are to precisely identify their molecular structures and catalytic sites, and understand their intrinsic mechanisms. The development of computational technologies will also be an important guide toward realizing high-performance GDY-based catalysts.

Acknowledgements

This work was supported by the National Nature Science Foundation of China (21790050, 21790051), the National Key Research and Development Project of China (2016YFA0200104), and the Key Program of the Chinese Academy of Sciences (QYZDY-SSW-SLH015).

Conflict of Interest

The authors declare no conflict of interest.

Keywords

graphdiyne, metal-free catalysts, oxygen reduction reaction, photocatalysts, water splitting

Received: June 14, 2018
Revised: July 10, 2018
Published online: September 27, 2018

[1] M. G. Walter, E. L. Warren, J. R. McKone, S. W. Boettcher, Q. Mi, E. A. Santori, N. S. Lewis, *Chem. Rev.* **2010**, *110*, 6446.
[2] X. Chen, S. Shen, L. Guo, S. S. Mao, *Chem. Rev.* **2010**, *110*, 6503.
[3] E. Perez-Gallent, G. Marcandalli, M. C. Figueiredo, F. Calle-Vallejo, M. T. M. Koper, *J. Am. Chem. Soc.* **2017**, *139*, 16412.
[4] M. Borghei, J. Lehtonen, L. Liu, O. J. Rojas, *Adv. Mater.* **2018**, *30*, 1703691.
[5] H. Wang, T. Maiyalagan, X. Wang, *ACS Catal.* **2012**, *2*, 781.
[6] I. E. L. Stephens, A. S. Bondarenko, U. Gronbjerg, J. Rossmeisl, I. Chorkendorff, *Energy Environ. Sci.* **2012**, *5*, 6744.
[7] B. Winther-Jensen, D. R. MacFarlane, *Energy Environ. Sci.* **2011**, *4*, 2790.
[8] G. Zhang, G. Wang, Y. Liu, H. Liu, J. Qu, J. Li, *J. Am. Chem. Soc.* **2016**, *138*, 14686.
[9] P. Cai, J. Huang, J. Chen, Z. Wen, *Angew. Chem., Int. Ed.* **2017**, *56*, 4858.
[10] P. Cai, Y. Li, G. Wang, Z. Wen, *Angew. Chem., Int. Ed.* **2018**, *57*, 3910.
[11] G. Wu, P. Zelenay, *Acc. Chem. Res.* **2013**, *46*, 1878.
[12] L. Dai, *Acc. Chem. Res.* **2013**, *46*, 31.
[13] C. Su, K. P. Loh, *Acc. Chem. Res.* **2013**, *46*, 2275.
[14] C. Tang, Q. Zhang, *Adv. Mater.* **2017**, *29*, 1604103.
[15] L. Wang, A. Ambrosi, M. Pumera, *Angew. Chem., Int. Ed.* **2013**, *52*, 13818.

[16] J. Masa, W. Xia, M. Muhler, W. Schuhmann, *Angew. Chem., Int. Ed.* **2015**, *54*, 10102.
[17] V. Georgakilas, J. A. Perman, J. Tucek, R. Zboril, *Chem. Rev.* **2015**, *115*, 4744.
[18] R. L. McCreery, *Chem. Rev.* **2008**, *108*, 2646.
[19] D. S. Su, S. Perathoner, G. Centi, *Chem. Rev.* **2013**, *113*, 5782.
[20] G. Li, Y. Li, H. Liu, Y. Guo, Y. Li, D. Zhu, *Chem. Commun.* **2010**, *46*, 3256.
[21] Y. Li, L. Xu, H. Liu, Y. Li, *Chem. Soc. Rev.* **2014**, *43*, 2572.
[22] Z. Jia, Y. Li, Z. Zuo, H. Liu, C. Huang, Y. Li, *Acc. Chem. Res.* **2017**, *50*, 2470.
[23] X. Gao, H. Ren, J. Zhou, R. Du, C. Yin, R. Liu, H. Peng, L. Tong, Z. Liu, J. Zhang, *Chem. Mater.* **2017**, *29*, 5777.
[24] J. Xiao, J. Shi, H. Liu, Y. Xu, S. Lv, Y. Luo, D. Li, Q. Meng, Y. Li, *Adv. Energy Mater.* **2015**, *5*, 1401943.
[25] C. Kuang, G. Tang, T. Jiu, H. Yang, H. Liu, B. Li, W. Luo, X. Li, W. Zhang, F. Lu, J. Fang, Y. Li, *Nano Lett.* **2015**, *15*, 2756.
[26] C. Lu, Y. Yang, J. Wang, R. Fu, X. Zhao, L. Zhao, Y. Ming, Y. Hu, H. Lin, X. Tao, Y. Li, W. Chen, *Nat. Commun.* **2018**, *9*, 752.
[27] J. Xie, N. Wang, X. Dong, C. Wang, Z. Du, L. Mei, Y. Yong, C. Huang, Y. Li, Z. Gu, Y. Zhao, *ACS Appl. Mater. Interfaces* **2018**, https://doi.org/10.1021/acsami.1028b00949.
[28] H. Shang, Z. Zuo, L. Yu, F. Wang, F. He, Y. Li, *Adv. Mater.* **2018**, *30*, e1801459.
[29] S. Li, Y. Chen, H. Liu, Y. Wang, L. Liu, F. Lv, Y. Li, S. Wang, *Chem. Mater.* **2017**, *29*, 6087.
[30] Y. Xue, B. Huang, Y. Yi, Y. Guo, Z. Zuo, Y. Li, Z. Jia, H. Liu, Y. Li, *Nat. Commun.* **2018**, *9*, 1460.
[31] H. Yu, Y. Xue, L. Hui, C. Zhang, Y. Li, Z. Zuo, Y. Zhao, Z. Li, Y. Li, *Adv. Mater.* **2018**, *30*, e1707082.
[32] P. Siemsen, R. C. Livingston, F. Diederich, *Angew. Chem., Int. Ed.* **2000**, *39*, 2632.
[33] F. Diederich, *Nature* **1994**, *369*, 199.
[34] C. Ge, J. Chen, S. Tang, Y. Du, N. Tang, *ACS Appl. Mater. Interfaces* **2018**, https://doi.org/10.1021/acsami.1028b03413.
[35] C. Huang, Y. Li, *Acta Phys. Chim. Sin.* **2016**, *32*, 1314.
[36] H. Shang, Z. Zuo, L. Li, F. Wang, H. Liu, Y. Li, Y. Li, *Angew. Chem., Int. Ed.* **2018**, *57*, 774.
[37] R. Matsuoka, R. Sakamoto, K. Hoshiko, S. Sasaki, H. Masunaga, K. Nagashio, H. Nishihara, *J. Am. Chem. Soc.* **2017**, *139*, 3145.
[38] J. He, N. Wang, Z. Cui, H. Du, L. Fu, C. Huang, Z. Yang, X. Shen, Y. Yi, Z. Tu, Y. Li, *Nat. Commun.* **2017**, *8*, 1172.
[39] Z. Jia, Z. Zuo, Y. Yi, H. Liu, D. Li, Y. Li, Y. Li, *Nano Energy* **2017**, *33*, 343.
[40] R. Matsuoka, R. Toyoda, R. Shiotsuki, N. Fukui, K. Wada, H. Maeda, R. Sakamoto, S. Sasaki, H. Masunaga, K. Nagashio, H. Nishihara, *ACS Appl. Mater. Interfaces* **2018**, https://doi.org/10.1021/acsami.1028b00743.
[41] X. Kan, Y. Ban, C. Wu, Q. Pan, H. Liu, J. Song, Z. Zuo, Z. Li, Y. Zhao, *ACS Appl. Mater. Interfaces* **2018**, *10*, 53.
[42] B. Cirera, Y. Q. Zhang, J. Bjork, S. Klyatskaya, Z. Chen, M. Ruben, J. V. Barth, F. Klappenberger, *Nano Lett.* **2014**, *14*, 1891.
[43] Y. Q. Zhang, N. Kepcija, M. Kleinschrodt, K. Diller, S. Fischer, A. C. Papageorgiou, F. Allegretti, J. Bjork, S. Klyatskaya, F. Klappenberger, M. Ruben, J. V. Barth, *Nat. Commun.* **2012**, *3*, 1286.
[44] R. Du, N. Zhang, H. Xu, N. Mao, W. Duan, J. Wang, Q. Zhao, Z. Liu, J. Zhang, *Adv. Mater.* **2014**, *26*, 8053.
[45] J. Zhou, X. Gao, R. Liu, Z. Xie, J. Yang, S. Zhang, G. Zhang, H. Liu, Y. Li, J. Zhang, Z. Liu, *J. Am. Chem. Soc.* **2015**, *137*, 7596.
[46] G. Li, Y. Li, X. Qian, H. Liu, H. Lin, N. Chen, Y. Li, *J. Phys. Chem. C* **2011**, *115*, 2611.
[47] Z. Zuo, H. Shang, Y. Chen, J. Li, H. Liu, Y. Li, Y. Li, *Chem. Commun.* **2017**, *53*, 8074.
[48] N. Wang, J. He, Z. Tu, Z. Yang, F. Zhao, X. Li, C. Huang, K. Wang, T. Jiu, Y. Yi, Y. Li, *Angew. Chem., Int. Ed.* **2017**, *56*, 10740.
[49] Y. Yang, X. Xu, *Comput. Mater. Sci.* **2012**, *61*, 83.
[50] Q. Yue, S. Chang, J. Kang, S. Qin, J. Li, *J. Phys. Chem. C* **2013**, *117*, 14804.
[51] J. Li, Z. Xie, Y. Xiong, Z. Li, Q. Huang, S. Zhang, J. Zhou, R. Liu, X. Gao, C. Chen, L. Tong, J. Zhang, Z. Liu, *Adv. Mater.* **2017**, *29*, 1700421.
[52] N. Wang, X. Li, Z. Tu, F. Zhao, J. He, Z. Guan, C. Huang, Y. Yi, Y. Li, *Angew. Chem., Int. Ed.* **2018**, *57*, 3968.
[53] H. Shang, Z. Zuo, H. Zheng, K. Li, Z. Tu, Y. Yi, H. Liu, Y. Li, Y. Li, *Nano Energy* **2018**, *44*, 144.
[54] Z. Yang, X. Shen, N. Wang, J. He, X. Li, X. Wang, Z. Hou, K. Wang, J. Gao, T. Jiu, C. Huang, *ACS Appl. Mater. Interfaces* **2018**, https://doi.org/10.1021/acsami.1028b01823.
[55] Q. Pan, H. Liu, Y. Zhao, S. Chen, B. Xue, X. Kan, X. Huang, J. Liu, Z. Li, *ACS Appl. Mater. Interfaces* **2018**, https://doi.org/10.1021/acsami.1028b03311.
[56] S. Zhang, H. Du, J. He, C. Huang, H. Liu, G. Cui, Y. Li, *ACS Appl. Mater. Interfaces* **2016**, *8*, 8467.
[57] R. Liu, H. Liu, Y. Li, Y. Yi, X. Shang, S. Zhang, X. Yu, S. Zhang, H. Cao, G. Zhang, *Nanoscale* **2014**, *6*, 11336.
[58] C. Li, X. Lu, Y. Han, S. Tang, Y. Ding, R. Liu, H. Bao, Y. Li, J. Luo, T. Lu, *Nano Res.* **2018**, *11*, 1714.
[59] J. Zhong, J. Wang, J.-G. Zhou, B.-H. Mao, C.-H. Liu, H.-B. Liu, Y.-L. Li, T.-K. Sham, X.-H. Sun, S.-D. Wang, *J. Phys. Chem. C* **2013**, *117*, 5931.
[60] G. F. Luo, X. M. Qian, H. B. Liu, R. Qin, J. Zhou, L. Z. Li, Z. X. Gao, E. G. Wang, W. N. Mei, J. Lu, Y. L. Li, S. Nagase, *Phys. Rev. B* **2011**, *84*, 075439.
[61] J. Koo, M. Park, S. Hwang, B. Huang, B. Jang, Y. Kwon, H. Lee, *Phys. Chem. Chem. Phys.* **2014**, *16*, 8935.
[62] M. Hu, Y. Pan, K. Luo, J. He, D. Yu, B. Xu, *Carbon* **2015**, *91*, 518.
[63] G. Luo, Q. Zheng, W.-N. Mei, J. Lu, S. Nagase, *J. Phys. Chem. C* **2013**, *117*, 13072.
[64] S. Pari, A. Cuéllar, B. M. Wong, *J. Phys. Chem. C* **2016**, *120*, 18871.
[65] H. Bu, M. Zhao, H. Zhang, X. Wang, Y. Xi, Z. Wang, *J. Phys. Chem. A* **2012**, *116*, 3934.
[66] N. Ketabi, T. M. Tolhurst, B. Leedahl, H. B. Liu, Y. L. Li, A. Moewes, *Carbon* **2017**, *123*, 1.
[67] M. Long, L. Tang, D. Wang, Y. Li, Z. Shuai, *ACS Nano* **2011**, *5*, 2593.
[68] H. Tong, S. Ouyang, Y. Bi, N. Umezawa, M. Oshikiri, J. Ye, *Adv. Mater.* **2012**, *24*, 229.
[69] J. Ran, M. Jaroniec, S. Z. Qiao, *Adv. Mater.* **2018**, *30*, 1704649.
[70] Y. Jiao, Y. Zheng, P. Chen, M. Jaroniec, S. Z. Qiao, *J. Am. Chem. Soc.* **2017**, *139*, 18093.
[71] C. Y. Lin, D. Zhang, Z. Zhao, Z. Xia, *Adv. Mater.* **2018**, *30*, 1703646.
[72] G. M. Psofogiannakis, G. E. Froudakis, *J. Phys. Chem. C* **2012**, *116*, 19211.
[73] H. Jin, A. M. Plonka, J. B. Parise, N. S. Goroff, *CrystEngComm* **2013**, *15*, 3106.
[74] J. W. Lauher, F. W. Fowler, N. S. Goroff, *Acc. Chem. Res.* **2008**, *41*, 1215.
[75] R. Xu, W. B. Schweizer, H. Frauenrath, *J. Am. Chem. Soc.* **2008**, *130*, 11437.
[76] Y. Xu, M. D. Smith, M. F. Geer, P. J. Pellechia, J. C. Brown, A. C. Wibowo, L. S. Shimizu, *J. Am. Chem. Soc.* **2010**, *132*, 5334.
[77] X. F. Gao, X. M. Shen, *Carbon* **2017**, *125*, 536.
[78] Y. Han, Y. G. Wang, W. Chen, R. Xu, L. Zheng, J. Zhang, J. Luo, R. A. Shen, Y. Zhu, W. C. Cheong, C. Chen, Q. Peng, D. Wang, Y. Li, *J. Am. Chem. Soc.* **2017**, *139*, 17269.
[79] B. K. Das, D. Sen, K. K. Chattopadhyay, *Carbon* **2016**, *105*, 330.
[80] B. T. Kang, H. Shi, S. Wu, W. Zhao, H. Q. Ai, J. Y. Lee, *Carbon* **2017**, *123*, 415.

[81] B. K. Das, D. Sen, K. K. Chattopadhyay, *Phys. Chem. Chem. Phys.* **2016**, *18*, 2949.
[82] X. K. Kong, Y. M. Huang, Q. C. Liu, *Carbon* **2017**, *123*, 558.
[83] S. Satyapal, J. Petrovic, C. Read, G. Thomas, G. Ordaz, *Catal. Today* **2007**, *120*, 246.
[84] P. A. Berseth, A. G. Harter, R. Zidan, A. Blomqvist, C. M. Araújo, R. H. Scheicher, R. Ahuja, P. Jena, *Nano Lett.* **2009**, *9*, 1501.
[85] B. Sakintuna, F. Lamari-Darkrim, M. Hirscher, *Int. J. Hydrogen Energy* **2007**, *32*, 1121.
[86] B. Bogdanović, M. Felderhoff, A. Pommerin, F. Schüth, N. Spielkamp, *Adv. Mater.* **2006**, *18*, 1198.
[87] S. C. Shekar, R. S. Swathi, *J. Phys. Chem. C* **2015**, *119*, 8912.
[88] D. W. Ma, T. X. Li, Q. G. Wang, G. Yang, C. Z. He, B. Y. Ma, Z. S. Lu, *Carbon* **2015**, *95*, 756.
[89] Z.-Z. Lin, *Carbon* **2016**, *108*, 343.
[90] H. Z. Yu, A. J. Du, Y. Song, D. J. Searles, *J. Phys. Chem. C* **2013**, *117*, 21643.
[91] P. Wu, P. Du, H. Zhang, C. X. Cai, *Phys. Chem. Chem. Phys.* **2014**, *16*, 5640.
[92] E. H. Song, Z. Wen, Q. Jiang, *J. Phys. Chem. C* **2011**, *115*, 3678.
[93] F. Li, J. Zhao, Z. Chen, *J. Phys. Chem. C* **2012**, *116*, 2507.
[94] C. Liu, Y. Tan, S. Lin, H. Li, X. Wu, L. Li, Y. Pei, X. C. Zeng, *J. Am. Chem. Soc.* **2013**, *135*, 2583.
[95] M. A. Petersen, S. J. Jenkins, D. A. King, *J. Phys. Chem. B* **2006**, *110*, 11962.
[96] Y.-H. Lu, M. Zhou, C. Zhang, Y.-P. Feng, *J. Phys. Chem. C* **2009**, *113*, 20156.
[97] J. He, S. Y. Ma, P. Zhou, C. X. Zhang, C. He, L. Z. Sun, *J. Phys. Chem. C* **2012**, *116*, 26313.
[98] L. Wang, Y. Wan, Y. Ding, S. Wu, Y. Zhang, X. Zhang, G. Zhang, Y. Xiong, X. Wu, J. Yang, H. Xu, *Adv. Mater.* **2017**, *29*, 1702428.
[99] T. Zhang, Y. Hou, V. Dzhagan, Z. Liao, G. Chai, M. Löffler, D. Olianas, A. Milani, S. Xu, M. Tommasini, D. R. T. Zahn, Z. Zheng, E. Zschech, R. Jordan, X. Feng, *Nat. Commun.* **2018**, *9*, 1140.
[100] D. Schwarz, Y. Noda, J. Klouda, K. Schwarzova-Peckova, J. Tarabek, J. Rybacek, J. Janousek, F. Simon, M. V. Opanasenko, J. Cejka, A. Acharjya, J. Schmidt, S. Selve, V. Reiter-Scherer, N. Severin, J. P. Rabe, P. Ecorchard, J. He, M. Polozij, P. Nachtigall, M. J. Bojdys, *Adv. Mater.* **2017**, *29*, 1703399.
[101] R. Godin, Y. Wang, M. A. Zwijnenburg, J. Tang, J. R. Durrant, *J. Am. Chem. Soc.* **2017**, *139*, 5216.
[102] Q. Han, Z. H. Cheng, J. Gao, Y. Zhao, Z. P. Zhang, L. M. Dai, L. T. Qu, *Adv. Funct. Mater.* **2017**, *27*, 1606352.
[103] H. Kasap, C. A. Caputo, B. C. M. Martindale, R. Godin, V. W.-H. Lau, B. V. Lotsch, J. R. Durrant, E. Reisner, *J. Am. Chem. Soc.* **2016**, *138*, 9183.
[104] W.-J. Ong, L.-L. Tan, Y. H. Ng, S.-T. Yong, S.-P. Chai, *Chem. Rev.* **2016**, *116*, 7159.
[105] Y.-Y. Han, X.-L. Lu, S.-F. Tang, X.-P. Yin, Z.-W. Wei, T.-B. Lu, *Adv. Energy Mater.* **2018**, *8*, 1702992.
[106] X. Gao, J. Li, R. Du, J. Zhou, M. Y. Huang, R. Liu, J. Li, Z. Xie, L. Z. Wu, Z. Liu, J. Zhang, *Adv. Mater.* **2017**, *29*, 1605308.
[107] Q. Lv, W. Y. Si, Z. Yang, N. Wang, Z. Y. Tu, Y. P. Yi, C. S. Huang, L. Jiang, M. J. Zhang, J. J. He, Y. Z. Long, *ACS Appl. Mater. Interfaces* **2017**, *9*, 29744.
[108] S. Yang, R. E. Bachman, X. Feng, K. Mullen, *Acc. Chem. Res.* **2013**, *46*, 116.
[109] S. Fujii, T. Enoki, *Acc. Chem. Res.* **2012**, *46*, 2202.
[110] Y. Xue, Y. Guo, Y. Yi, Y. Li, H. Liu, D. Li, W. Yang, Y. Li, *Nano Energy* **2016**, *30*, 858.
[111] J. Jin, M. Guo, J. Liu, J. Liu, H. Zhou, J. Li, L. Wang, H. Liu, Y. Li, Y. Zhao, C. Chen, *ACS Appl. Mater. Interfaces* **2018**, *10*, 8436.
[112] Y. Dang, W. Y. Guo, L. M. Zhao, H. Y. Zhu, *ACS Appl. Mater. Interfaces* **2017**, *9*, 30002.
[113] R. Liu, X. Gao, J. Zhou, H. Xu, Z. Li, S. Zhang, Z. Xie, J. Zhang, Z. Liu, *Adv. Mater.* **2017**, *29*, 1604665.
[114] J. Zhou, Z. Xie, R. Liu, X. Gao, J. Li, Y. Xiong, L. Tong, J. Zhang, Z. Liu, *ACS Appl. Mater. Interfaces* **2018**, https://doi.org/10.1021/acsami.1028b02612.
[115] X. Qian, H. Liu, C. Huang, S. Chen, L. Zhang, Y. Li, J. Wang, Y. Li, *Sci. Rep.* **2015**, *5*, 7756.
[116] P. Pachfule, A. Acharjya, J. Roeser, T. Langenhahn, M. Schwarze, R. Schomacker, A. Thomas, J. Schmidt, *J. Am. Chem. Soc.* **2018**, *140*, 1423.
[117] L. Luo, D. Resch, C. Wilhelm, C. N. Young, G. P. Halada, R. J. Gambino, C. P. Grey, N. S. Goroff, *J. Am. Chem. Soc.* **2011**, *133*, 19274.
[118] Y. R. Xue, J. F. Li, Z. Xue, Y. J. Li, H. B. Liu, D. Li, W. S. Yang, Y. L. Li, *ACS Appl. Mater. Interfaces* **2016**, *8*, 31083.
[119] Q. Li, W. Chen, H. Xiao, Y. Gong, Z. Li, L. Zheng, X. Zheng, W. Yan, W. C. Cheong, R. Shen, N. Fu, L. Gu, Z. Zhuang, C. Chen, D. Wang, Q. Peng, J. Li, Y. Li, *Adv. Mater.* **2018**, *30*, 1800588.
[120] J. Zhang, M. Ren, L. Wang, Y. Li, B. I. Yakobson, J. M. Tour, *Adv. Mater.* **2018**, *30*, 1707319.
[121] Y. Xue, Z. Zuo, Y. Li, H. Liu, Y. Li, *Small* **2017**, *13*, 1700936.
[122] J. Wang, W. Cui, Q. Liu, Z. Xing, A. M. Asiri, X. Sun, *Adv. Mater.* **2016**, *28*, 215.
[123] Y. Pan, R. Lin, Y. Chen, S. Liu, W. Zhu, X. Cao, W. Chen, K. Wu, W. C. Cheong, Y. Wang, L. Zheng, J. Luo, Y. Lin, Y. Liu, C. Liu, J. Li, Q. Lu, X. Chen, D. Wang, Q. Peng, C. Chen, Y. Li, *J. Am. Chem. Soc.* **2018**, *140*, 4218.
[124] Y. Cheng, S. Zhao, B. Johannessen, J. P. Veder, M. Saunders, M. R. Rowles, M. Cheng, C. Liu, M. F. Chisholm, R. De Marco, H. M. Cheng, S. Z. Yang, S. P. Jiang, *Adv. Mater.* **2018**, *30*, 1706287.